Clarification of mammalian cloacal morphogenesis using high-resolution episcopic microscopy

Yi Chen Huang [a], Fang Chen [b], Xue Li [a,*]

[a] Departments of Urology and Pathology, Boston Children's Hospital, and Department of Surgery, Harvard Medical School, 300 Longwood Avenue, Boston, MA 02115, USA
[b] Department of Urology, Shanghai Children's Hospital, Shanghai JiaoTong University, Shanghai 200062, China

ARTICLE INFO

ABSTRACT

The developmental process through which the cloaca transforms from one hollow structure to two separated urinary and digestive outlets remains controversial and speculative. Here, we use high-resolution episcopic microscopy to examine a comprehensive series of normal and mutant mouse cloaca in which the detailed 3-dimensional (3-D) morphological features are illuminated throughout the development. We provide evidence that the dorsal peri-cloacal mesenchyme (dPCM) remains stationary while other surrounding tissues grow towards it. This causes dramatic changes of spatial relationship among caudal structures and morphological transformation of the cloaca. The 3-D characterizations of *Dkk1* mutants reveal a hyperplastic defect of dPCM, which leads to a significant anterior shift of the caudal boundary of the cloaca, premature occlusion of the cloaca and, imperforate anus phenotype. Conversely, *Shh* knockout causes a severe hypoplastic defect of cloaca mesenchyme including dPCM and persistent cloaca. Collectively, these findings suggest that formation of the dPCM is critical for cloacal morphogenesis and furthermore, growth and movement of the mesenchymal tissues towards the dPCM lead to the cloaca occlusion and separation of the urinary and digestive outlets.

© 2015 Elsevier Inc. All rights reserved.

1. Introduction

The cloaca is a transient widening of the hindgut. It is divided during embryogenesis so that the digestive and urinary tracts of placental mammals exit the body separately. Abnormal cloaca development causes urogenital and anorectal malformations, which are among the most common forms of human birth defects. Despite extensive investigation, however, the process of mammalian cloacal morphogenesis remains a subject of controversy and speculation.

The century-old urorectal septum (URS)-based septation model offers the simplest interpretations. The model was primarily based on images of the midline sagittal sections, which give an impression of a septal structure, i.e. the URS, between the primitive hindgut and bladder. Rathke (1832) posited that the putative

bilateral plicae fuse to form the septum and divide the cloaca through a "zipper-like" process. Tourneux (1888), on the other hand, suggested that the septum descends like a "theater curtain" to separate the cloaca in the rostral-to-caudal direction. Many have attempted to experimentally test the septum-based hypotheses. For instance, Hynes and Fraher have performed a serial histological section analysis together with the computer-assisted three-dimensional (3-D) reconstruction and concluded that the presumptive URS is derived from the progressive median fusion of longitudinal folds, i.e. Rathke's plicae, on the lateral walls of the cloaca (Hynes and Fraher, 2004). However, using the similar approaches and scanning electron micrograph (SEM), several other investigators suggested that there is no evidence of the Rathke plicae nor the Tourneux fold in mouse (Penington and Hutson, 2003), rat (Kluth et al., 1995), pig or human embryos (Nievelstein et al., 1998; Paidas et al., 1999; van der Putte, 1986). The reason for the discrepancy is not entirely clear but the curved shape of the cloaca may render unambiguous description difficult in the absent of a complete set of 3-D images.

Closely related to cloaca morphogenesis is the caudal development during the secondary axis formation of the vertebrate body plan. After gastrulation, which establishes the primary body axis, vertebrate embryos grow substantially in length at the caudal end and at the same time undergo dramatic morphological

changes including rotation and repositioning of caudal and ventral structures (Hassoun et al., 2010; Muller and O'Rahilly, 2004; Tam, 1981; Wilson and Beddington, 1996). Characterization of a series of human embryos ranging from 25 to 54 days' gestation suggested that transformation of the cloaca is a passive process secondary to caudal development (Nievelstein et al., 1998; Paidas et al., 1999). This theory rejects the notion that the URS grows caudally in the direction of and fuses with the cloaca membrane (CM). It further suggests that the apparent decrease in distance between the URS and the CM is due to the caudal unfolding process, which passively changes the spatial relationship between the involved structures.

Because of the rapidly changing size, shape and spatial relationships among multiple structures during cloaca development, high quality serial 3-D images are required to fully appreciate the morphological complexity. Here, we use high-resolution episcopic microscope (HREM) technology (Mohun and Weninger, 2012a), which preserves and digitizes fine 3-D morphological features. This allows us to generate a series of 3-D "snapshots" of mouse cloaca, to create *de facto* live imaging of the entire process of cloacal morphogenesis and, to quantitative analyze size and dimensions of all structures involved. We provide evidence that the dorsal pericloacal mesenchyme (dPCM) demarcates the caudal boundary of the cloaca. During cloaca development, the dPCM remains stationary while other mesenchymal tissues surrounding the cloaca grow towards it. In this way, the cloaca is occluded and the remnant of the cloaca is displaced to the epithelial surface of the perineum. Results from this study also suggest that defects of the dPCM likely contribute to the pathogenesis of urogenital and anorectal anomalies. We believe that the serial high-resolution 3-D images generated herein will serve as a useful resource for studying human cloaca defects using mouse models.

2. Materials and methods

2.1. Animals

All animal studies were approved by the Institutional Animal Care and Use Committee at Boston Children's Hospital. C57Bl6 wild type mice are obtained from Charles River. *DKK1* and *Shh* mutant mice have been described previously (Guo et al., 2014). Image acquisition and processing protocols are included as supplementary data (Fig. S1).

2.2. High-resolution episcopic microscopy imaging

Block face images were captured using a procedure similar to that described (Mohun and Weninger, 2012b). Briefly, tissue blocks were mounted on a rotary microtome (Leica, RM2265). The stop position of after each rotation was kept constant. A stereo zoom microscope (Zeiss, Axio Zoom.V16) was mounted perpendicularly to the block surface. A digital camera (Hamamatsu Photonics K.K., C11440-10C) equipped with green fluorescent protein (GFP) filter cube set (excitation $470 +/- 20$ nm, dichroic 495 nm, emission $525 +/- 25$ nm) was used to capture images of the block face. Images (1920×1440 pixels) were scaled automatically from 1.5×1.5 μm/pixel to 3.6×3.6 μm/pixel (Zen pro 2012, Zeiss) depending on the size of embryos. Section thickness was set at 1.5 μm (e9.5 and e10.0), 2.0 μm (e10.5–e12.0) and 2.5 μm (e12.5–e13.5). Images were captured in grayscale mode. The exposure time was adjusted from 120 ms to 320 ms accordingly.

2.3. Image processing and data analysis

All images were inverted using Photoshop (Adobe, V13.0) and further converted to volume data using the 3-D visualization software (Amira V5.4.5). When loading the images, we included resolution and thickness into the text fields of the Voxel Size port to define the size of voxels, so that the scale of the reconstructed image accurately reflected the size of each specimen. In order to optimize the quality of the 3-D reconstructed images, we used the AlignSlices module to align the original 2-D images automatically and adjusted these manually where necessary. During this procedure, the Least-Squares alignment mode with default settings was applied. Subsequently, the 3-D views were generated using the Volren module. Using this whole mount image as a reference, we generated virtual sections through the embryo by the ObliqueSlice module. In this module, the section plane could be freely rotated and shifted. The Scale module was used to show the 2-D coordinates. A snapshot was taken in the Orthogonal Projection mode.

The somites were visualized both in sagittal and whole mount images. To determine the relative location (somite number) of the leading edges of each structure, we first established the midline sagittal view. We then created another planes perpendicular to the sagittal image to determine the corresponding somite. In order to visualize the cloacal lumen, we labeled the images manually in the Segmentation Editor using the LabelField module. We used the lasso and brush tools to label the lumen every three original 2-D slices. The Interpolate command was applied to label the intervening slices automatically. The labeling was inspected manually and adjusted if needed. Surface views of the cloacal lumen were visualized using the SurfaceGen module. To create video animations, we connected the CameraRotate module to the cloacal lumen, added the ObjectTranslate module to the sectional images, and generated flythrough videos by CameraPath module. These actions were edited with the DemoMaker Module. All videos were recorded into movie files using the MovieMaker module.

3. Results

3.1. 3-D overviews of mouse cloaca during morphogenesis

Mouse embryos were collected from a total of 9 separate developmental stages between day 9.5 (e9.5) or somite stage 25 (s25) and e13.5/s65, the period during which mouse cloaca is formed and transformed into the urogenital and the anorectal outflow tracts (Wang et al., 2013). To directly visualize the morphogenetic process, we generated 3-D HREM images from these embryos at all developmental stages (Figs. 1, S1 and S2, $n \geq 3$). Both vaginal plug date and somite number were used to better estimate embryo age. Important morphological features of the cloaca began to emerge from the 3-D images. At e9.5, an enlarged segment of the hindgut or the cloaca ended bluntly into the tail bud or the caudal eminence (Fig. 1A and a). The CM was detected at the ventrocaudal midline region of the hindgut (Fig. 1, yellow line and between two white arrowheads). There were no significant morphological changes of the hindgut during the next 12 hours with the exception of the tail gut formation (Fig. 1B and b). However, the cloaca began to distinguish itself morphologically starting at e10.5 (Fig. 1C and c). During the next 48 h, the large cloaca cavity was reduced to a thin tube at e12.5, the cloaca duct (CD) (Fig. 1C–G and c–g). At the same time, the primitive ventral urogenital and dorsal anorectal tracts emerged and were physically connected via the CD (Fig. 1G and g). Twelve hours later at e13.0 (Fig. 1H, h, I and i), the lumen of the CD narrowed significantly and the epithelial tube began to disintegrate. As the result, the urogenital and the anorectal tracts appeared to be separated completely. The actual fate of the CD is likely the ventral midline epithelial seam, *i.e.* the perineal and penile raphe (Seifert et al., 2008). This is the end stage of cloacal morphogenesis and
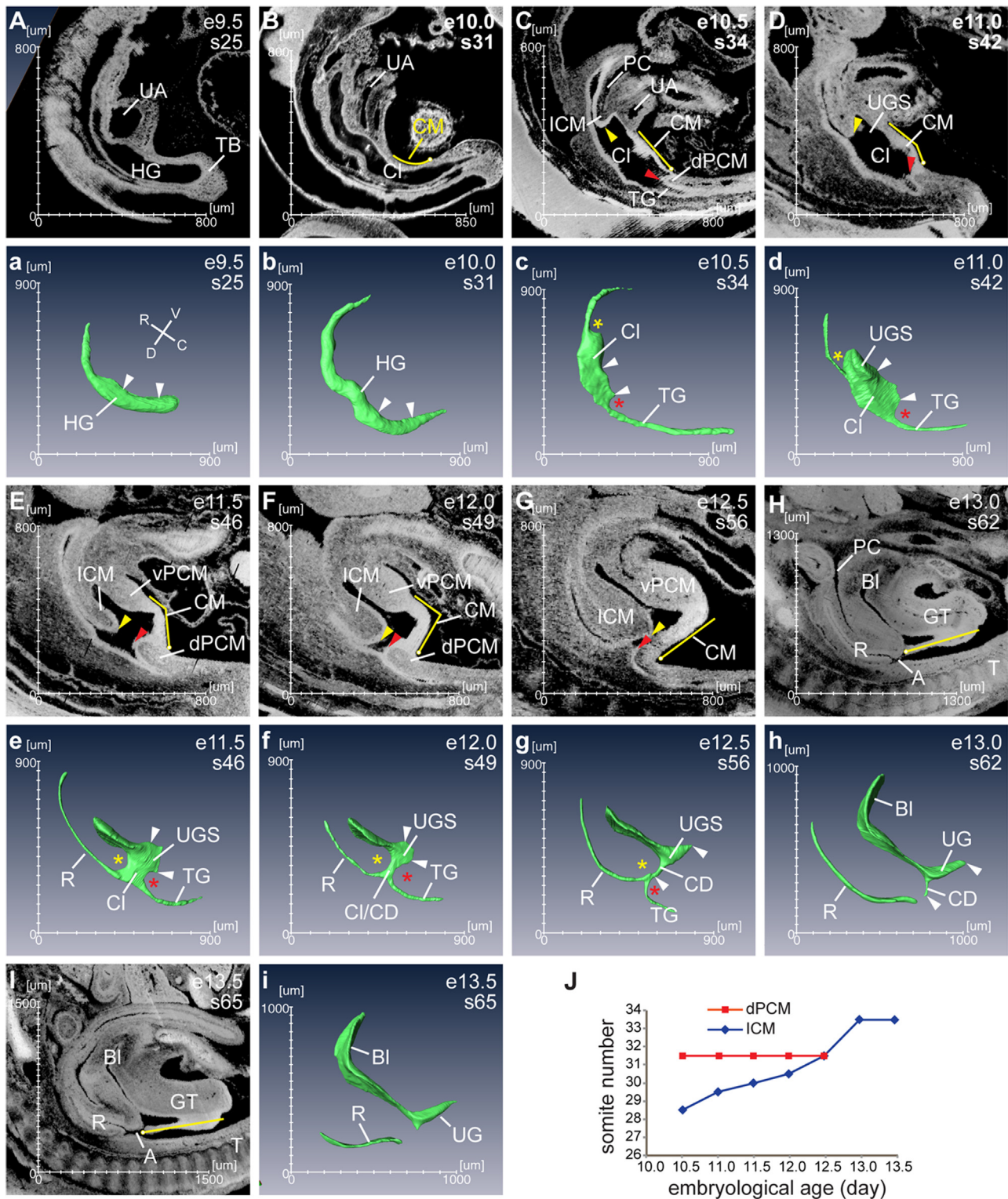
Fig. 1. Sagittal and 3-D views of the developing mouse cloaca. (A–I) The midline sagittal views of mouse cloaca from embryonic (e) day 9.5 to e13.5, or somatic (s) stage 25 to s65. The corresponding 3-D images of the hindgut are shown in a–i. All images are orientated in the same way as indicated in panel a. A, anus; bl, bladder; CD, cloacal duct; Cl, cloaca; CM, cloaca membrane; dPCM, dorsal pericloacal mesenchyme; GT, genital tubercle; HG, hindgut; ICM, intra-cloacal mesenchyme; PC, peritoneal cavity; R, rectum; T, tail; TB, tail bud; TG, tailgut; UA, umbilical artery; UG, urethral groove; UGS, urogenital sinus; vPCM, ventral peri-cloacal mesenchyme; yellow arrowhead, the leading edge of the ICM; red arrowhead, leading edge of the dPCM; yellow line, cloaca membrane; yellow asterisk, rostral cloaca indentation by the ICM; red asterisk, caudal cloaca indentation by the dPCM; white arrowheads, the rostrocaudal limits of the CM. (J) Graphical view of relative positions of the dPCM and the ICM.

the beginning of growth and differentiation of the urogenital and the anorectal tracts (Fig. 1H and I and h and i). Collectively, these findings show that the major morphological changes to mouse cloaca occur within two days between e10.5 and e12.5, which correspond to 28 and 40 days' gestation of human embryos, respectively.

Supplementary material related to this article can be found online at: http://dx.doi.org/%2010.1016/j.ydbio.2015.10.018.
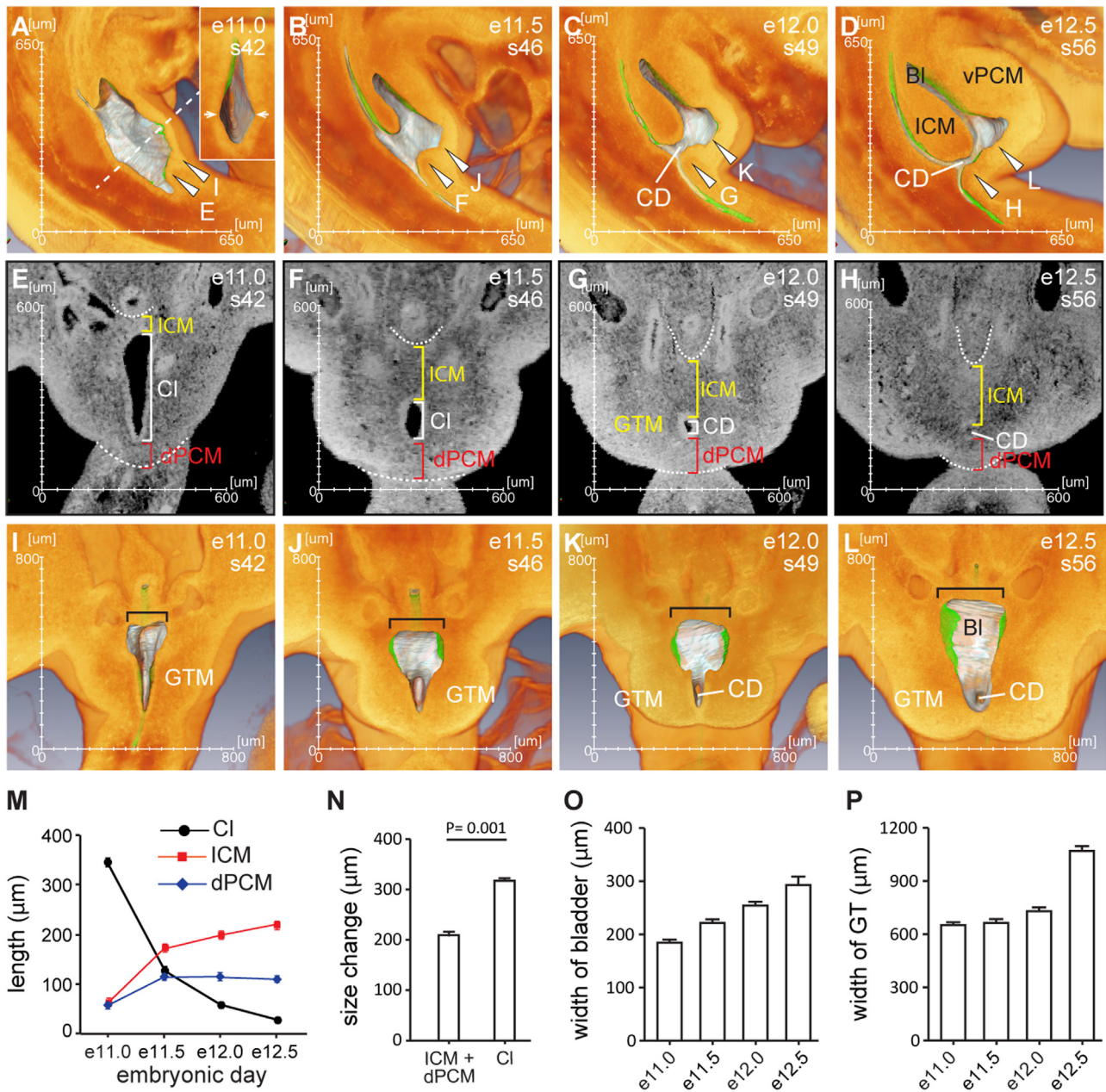
Fig. 2. The spatial relationships of structures involved in morphogenesis of the cloaca. (A–D) 3-D midline views of the sagittal half of embryos from e11.0 to e12.5. The endoderm epithelium including the cloaca was highlighted silver gray while the rest of the tissue was orange. When the endoderm was behind a layer of orange tissue, it appeared green. The inset in A shows a cross-section view from the dotted line. Arrowheads indicate planes of section for panels shown in E–L. (E–H) Coronal virtual sections taken from the plans shown in A–D. The dotted line highlights the shape of peritoneum and the caudal limit of the dPCM. (I–L) 3-D coronal views from the planes indicated in A–D. (M) Size of mesenchymal tissues as measured by length along the rostrocaudal axis shown in E–H. (N) Concurrent to the size increase of ICM and dPCM, the cloaca narrows significantly from e11.0 to e12.5. However, the overall size changes are significantly different. (O) Width of the primitive bladder indicated in I–L. (P) Width of the genital tubercle (GT), which indicates growth of the genital tubercle mesenchyme (GTM). See Fig. 1 for abbreviations.

3.2. Immobility of the dPCM changes the spatial relationships of the caudal structures

We next examined spatial relationships of the caudal structures surrounding the cloaca. At e10.5, the developing cloaca is sandwiched by the intra-cloacal mesenchyme (ICM) rostrally and the dPCM caudally (Fig. 1C, yellow and red arrowheads, respectively). It became clear on the 3-D images that these mesenchymal swellings dented the hindgut along the rostrocaudal axis (Fig. 1c, asterisks), such that the ICM and the dPCM demarcate the rostral and caudal boundaries of the cloaca, respectively. At this stage the cloaca can be distinguished from the developing colon and tail gut. The distance between the ICM and the dPCM along the

rostrocaudal axis was apparently decreased within the next two days (Figs. 1C–G and 2). To examine the relative position of the ICM and the dPCM, we used somites as points of reference as each somite has a defined position along the rostrocaudal body axis. At e10.5, the leading edge of the ICM was located at a position between somite 28 and 29 while the rostral edge of the dPCM was located between somite 31 and 32. As development proceeded, the leading edge of the ICM shifted caudally. In contrast, the dPCM remained at the same position. By e12.5, the ICM had reached to the same level as the dPCM, and the cloaca narrowed significantly to become the CD (Fig. 1G). The ventral pericloacal mesenchyme (vPCM) formed ventrally and became obvious at e11.5 (Figs. 1E and 2B). This is the same structure of the unpaired anlage of the dorsal

structure of the genital tubercle (Kluth et al., 2011). The leading edge of the vPCM also shifted caudally from a position of somite 30 at e11.0 to somite 32 at e12.5. The cloaca membrane (CM) is a ventral midline epithelial seam of the cloaca that is located at the juxtaposition between the two bilateral GTM tissues. The CM is anchored to the dPCM dorsally and the vPCM ventrally. Because the dPCM remains stationary, the CM appeared to be rotating around the dPCM during the outgrowth of GTM and vPCM and, was eventually displaced at the ventral side of the genital tubercle (yellow lines in Fig. 1C–I). Interestingly, the human fetus also undergoes a 150° counter-clockwise rotation of the caudal axis; and this rotation has been proposed to be responsible for passively dividing the cloaca (Paidas et al., 1999). Collectively, the dPCM remains at a fixed position while other mesenchymal tissues including the ICM, vPCM and GTM shift caudally towards and the non-mesenchymal tissue CM rotates around the dPCM. The unique feature of the dPCM, *i.e.* its immobility, alters the spatial relationship of all caudal structures involved in the cloacal morphogenesis.

3.3. Tissue growth and the caudle unfolding process reshape the cloaca

We next quantitatively examined changes of the overall dimensions of the cloaca during development. Both virtual sections and 3-D images were used to obtain accurate measurements (Fig. 2). As shown in Figs. 1 and 2, the rostrocaudal distance of the cloacal cavity decreased dramatically between e11.0 and e12.5 and concurrently, the primitive bladder began to emerge. The distance between the rostral and caudal edges of the cloacal cavity was approximately 341 μm at e11.0 but reduced to 26 μm at e12.5 ($\Delta=315$ μm, Fig. 2M). This was due, in part, to growth of the rostral and caudal mesenchymal tissues. For instance, the distance between the peritoneum and the cloaca dramatically increased from 62 μm at e11.0 to 217 μm at e12.5 ($\Delta=155$ μm, Fig. 2M), which suggests a significant growth of the ICM. The dPCM increased slightly during the same period from 53 μm to 107 μm ($\Delta=54$ μm). The overall size increase ($155+54=209$ μm) of the mesenchymal tissues differs significantly from the decrease ($\Delta=315$ μm) of the cloacal cavity (Fig. 2N, $p=0.001$), suggesting that morphogenesis of the cloaca also depends on other factor(s). A likely candidate is the caudal unfolding process described in human embryos (Nievelstein et al., 1998; Paidas et al., 1999), which may passively change the spatial relationship and contribute to the size reduction of the cloaca.

The primitive bladder was sandwiched by the growing ICM and vPCM and appeared to be a leaf-like flatten sac at e12.5. While the cloaca is shrinking, the primitive bladder expanded bilaterally. Its initial width was 182 μm at e11.0 but increased to 293 μm at e12.5 (Fig. 2I–L, black bracket, and 2O). The genital tubercle mesenchyme (GTM) initially resided bilaterally but shifted caudally to the cloaca (Fig. 2E–H). During the same one and half day period between e11.0 and e12.5, the GTM expanded significantly as width of the genital tubercle (GT) increased from 651 μm at e11.0 to 1070 μm at e12.5 (Fig. 2P). This correlated to the decrease of mediolateral distance of cloacal cavity and formation of the cloacal duct and the urethral groove. Collectively, these quantitative measurements suggest that morphogenesis of the cloaca depends on both active and passive mechanisms such as growth and the caudal unfolding process, respectively.

3.4. The Rathke plicae and Tourneux fold are not observed on 3-D HREM images

Unlike its appearance on the midline sagittal sections (Figs. 1 and 2), the cloaca was surrounded by a circular confluence

of mesenchymal tissues on coronal views instead of being divided by the ICM (Fig. 2E–K). At e11.0, the cloaca was shaped as a triangle when viewed coronally (Fig. 2E). The shape of triangle became an oval with a concave outline at e11.5, and a thin circular tube at e12.0 and e12.5. As reported previously (Penington and Hutson, 2003), the concave outline is not compatible with the existence of either the Rathke plicae or the Tourneux fold. To better visualize the inner surface of the cloacal cavity and minimize the possibility of being misled by 2-D images, embryos were bisected digitally to expose the inner surface of the cloaca (Fig. 2A–D and I–L). At e11.0, the lateral wall of the cloaca protruded outwardly instead of inwardly. This was particularly evident on a cross section overall view because the cloacal cavity exhibited a diamond shape (Fig. 2A, inset). We also performed a "flythrough" inside the cloaca at e11.5 to visualize topographic features of the lumen in its entirety and the video clearly indicated that the rostral and caudal surface exhibited a smooth concave outline (Fig. S3). We did not detect any obvious signs that may suggest the existence of the lateral fold, *i.e.* Rathke plicae or Tourneux fold, protruding into the cloacal cavity.

We also analyzed the entire serial sections throughout the cloaca from both the transverse and coronal directions of e11.5 embryos, which failed to detect sign of protrusion (Figs. 3, S4 and S5). Specifically, the coronal views of e11.5 through cloaca revealed an oval shape (Figs. 2F and S4). Similarly, the cloaca exhibited a concave shape on most transverse sections (Figs. 3D and S5). When the section planes were away from the cloaca, however, the primitive bladder appeared to be separated physically from the rectum by the ICM (Fig. 3A and B), and very few sections at the most rostral limit of the cloacal cavity appeared to have the protrusion-like shape (Fig. 3C). This feature is often been cited as evidence of the Rathke plicae. Intriguingly, similar appearance was also observed when sections were taken at the most caudal end of the cloaca (Fig. 3E and F), suggesting that the appearance is not unique to the rostral region of the cloaca where the proposed Rathke plicae and Tourneux fold are. Given that we did not observe any structure protruding into the inner cloacal cavity (Fig. 2A–D), and the cloaca has an overall concaved shape (Fig. 2E–H), we suspect that the appearance is simply the 2-D impression of a curved 3-D structure. In support of this notion, Penington and Hutson stated "there was no septum, as it is usually defined. There was no evidence of any process of fusion occurring between the 2 lateral folds within the lumen of the cloaca (Penington and Hutson, 2003)."

3.5. Malformations of the PCM cause the urogenital and anorectal birth defects

Our observations suggest that formation of the dPCM is important for cloacal morphogenesis. To test this possibility, we examined *Shh* (Mo et al., 2001) and *Dkk1* (Guo et al., 2014) mouse mutants since they display persistent cloaca and imperforate anus phenotypes, respectively. In addition, *Dkk1* is a potent inhibitor of the canonical *Wnt* signal pathway, which synergistically interacts with the *Shh* pathway to regulate cloacal morphogenesis and genital tubercle development (Lin et al., 2008, 2009; Miyagawa et al., 2009). Four different stages of *Dkk1* mutant embryos and two stages of *Shh* mutants were analyzed (Fig. 4 and S6). High-resolution 3-D images were generated and compared with age-matched wild type controls. As shown in Fig. 4E, the caudal indentation of the cloaca created by formation of the dPCM was much more pronounced in *Dkk1* mutants at e11.5. The rostrocaudal length of dPCM was 166 m in *Dkk1* mutants, which is significantly longer than wild type controls (115 μm) (Fig. S7, $p=0.006$). The size of *Dkk1* mutant cloaca (51 μm) was also significantly smaller than wild type control (125 μm, $p=0.0002$, Fig.
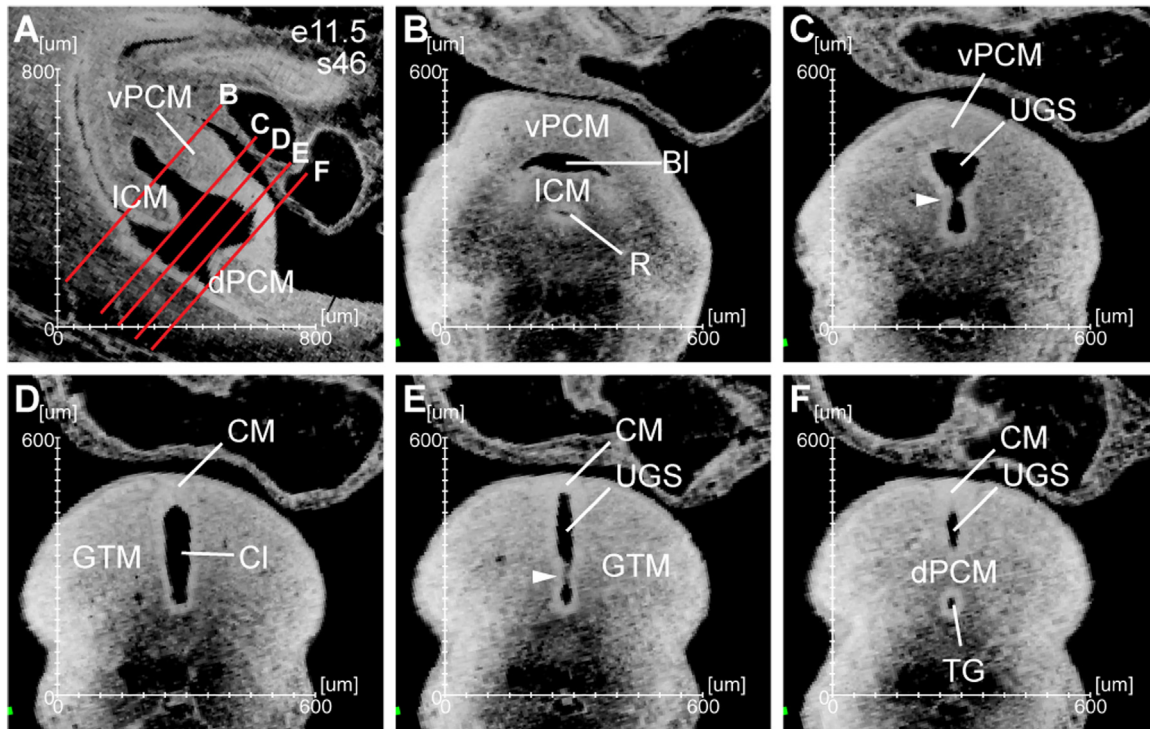
Fig. 3. Representative virtual sections throughout the cloaca. (A) A midline sagittal section from an e11.5 embryo. (B–F) The cross views of the cloaca from section planes shown in A (red lines). Arrowhead, features that are often cited as the Rathke plicae. Please see Fig. 1 for the abbreviations.

S7). The CM was shorter or almost undetectable at e11.5. The mutant ICM (170 μm) and GTM (639 μm), on the other hand, were comparable to controls (173 μm, $p=0.68$ and 668 μm, $p=0.11$, respectively, Fig. S7). A flythrough video inside *Dkk1* mutant cloaca further confirmed these observations including the abnormally large dPCM and a shortened CM (Fig. S8). Collectively, the quantitative measurements of HREM 3-D images support the previous report that the dPCM is hyperplastic in *Dkk1* mutants (Guo et al., 2014). In addition, these observations further suggest that the caudal boundary of the cloaca has shifted rostrally in *Dkk1* mutants and consequently, results in premature occlusion of the cloaca and imperforate anus phenotype.

In contrast to *Dkk1* mutants, severe hypoplastic growth of the dPCM was observed in *Shh* mutants (Fig. 4I–L). Formation of the ICM and the dPCM was observed initially at e10.5 in *Shh* mutants (Fig. S6E). However, both of these mesenchymal structures were significantly underdeveloped at e11.5 (Fig. 4I–K and S6F). The dPCM of *Shh* mutants was 77 μm, a 33% reduction when compared to wild type controls ($p=0.003$, Fig. S7). As a consequence, the expected caudal indentation was not observed at e11.5 (Fig. 4I). The ICM in *Shh* mutants was apparently reduced at this stage as well. The exact distance between the peritoneum and the cloaca could not be measured because it was not possible to unambiguous identify the peritoneum of Shh mutants. Consistent with the critical role of *Shh* in genital tubercle development (Lin et al., 2009; Miyagawa et al., 2009; Seifert et al., 2009), the overall width of GT from $Shh^{-/-}$ embryos at e11.5 was about 484 μm, which is significantly smaller than wild type controls (668 μm, $p=0.0004$, Fig. 4K, L and S7). Concordantly, *Shh* mutant cloaca was wider along the rostrocaudal and mediolateral axes, likely due to the hypoplastic defects of the surrounding mesenchymal tissues (Fig. 4K and 4L). Thus, growth of the caudal mesenchymal tissues depends on the *Shh* signaling.

4. Discussion

Morphogenesis of the cloaca is the result of dynamic changes of the spatial relationships among the involved mesenchymal and epithelial structures. Depending on the point of reference or the plane of view, one may derive different or even opposing models. Digitized HREM 3-D images offer the freedom to examine all involved structures using each other as well as independent landmark as references. By analyzing serial 3-D images of the cloaca throughout the development, we have begun to clarify major aspects of the cloaca morphogenetic process. The 3-D images collected herein will be a useful resource for future studies of the embryological and molecular basis of urogenital and anorectal birth defects.

It is generally accepted that the cloacal endoderm plays a critical role in growth and patterning of the surrounding mesenchyme, which feedback regulates morphogenesis of the cloaca. The classical septation model emphasizes the importance of mesenchymal cells, *i.e.* the ICM resided in the URS (Rathke, 1832; Tourneux, 1888). We prefer to use the term ICM instead of URS for three reasons. First, there is no comparable septal structure in the definitive anogenital region and importantly, the perineal stroma that separates the urinary and digestive outlets originates from mesenchymal cells surrounding the cloaca membrane (CM) (Wang et al., 2011, 2013). Second, the URS structure is only obvious on the midline sagittal sections but barely detectable on other section planes. Instead of an anatomically distinct structure, it is the continuum of mesenchyme surrounding the cloaca (Wang et al., 2011). Third, the term URS implies explicitly that it functions as a septum. On the other hand, ICM is simply an anatomic description thereby less contentious. The model proposed by van der Putte focuses on the mesenchyme located at the caudal boundary of the cloaca, *i.e.* the dPCM (van der Putte, 1986). Paidas et al. (1999) suggest that repositioning rather than relative growth of each mesenchymal tissue is essential to transforming the cloaca. The
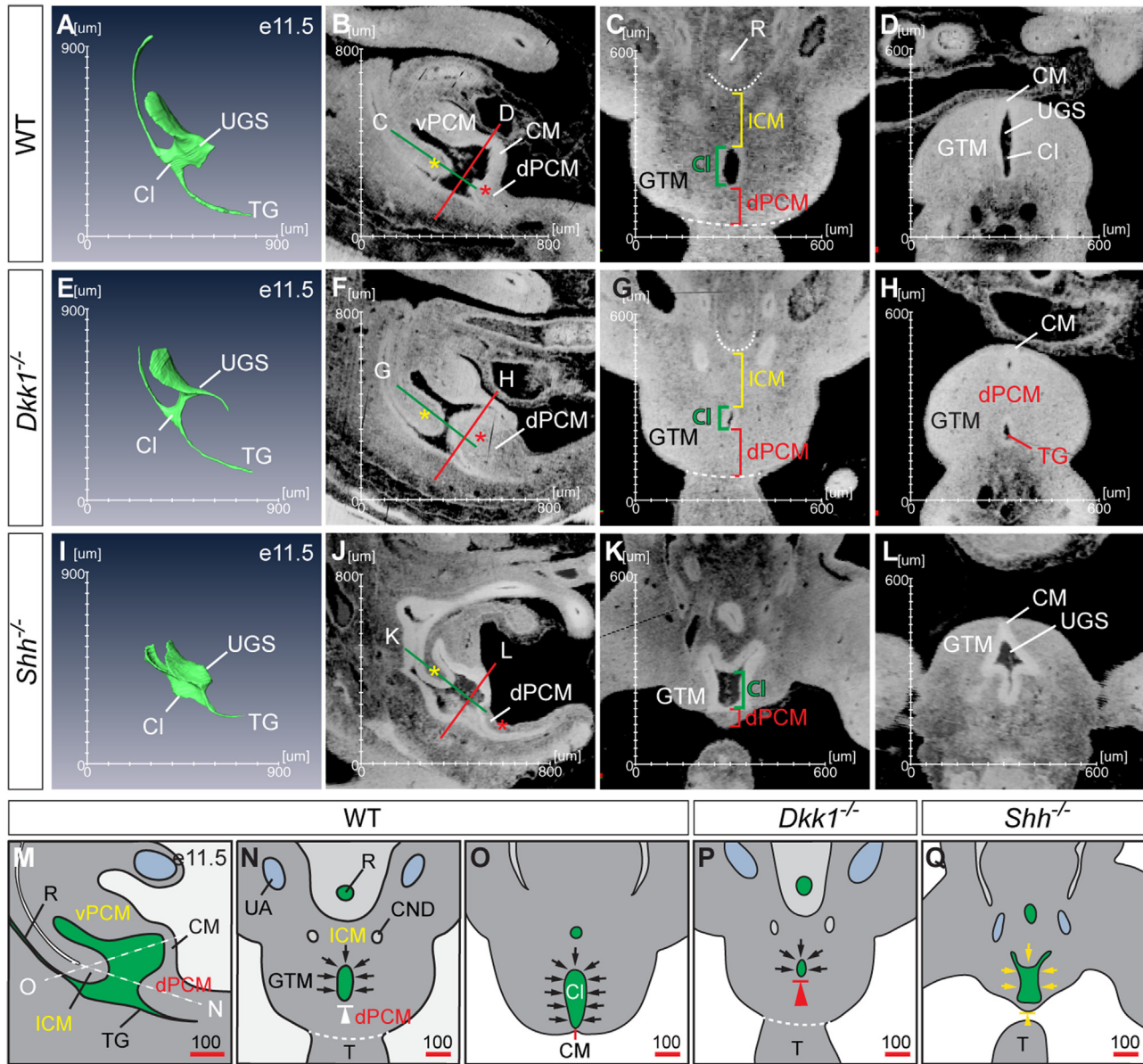
Fig. 4. The dPCM is critical for cloacal morphogenesis. Comparisons between wild type (A–D), $Shh^{-/-}$ (E–H) and $Dkk1^{-/-}$ (I–L) embryos at e11.5 suggest that formation of the dPCM is critical in separating the urinary and digestive tracts. Yellow asterisk, the ICM; red asterisk, the dPCM. Red and green lines indicated planes of sections shown in the corresponding panels. (M–N) Schematic diagrams of the wild type e11.5 cloaca from the midline sagittal (M), coronal (N) and cross (O) planes. White dash lines indicate the planes of sections shown in N and O. The proposed occlusion model suggests that reposition or growth of the surrounding mesenchymal tissues (*i.e.* ICM, vPCM and GTM, black arrows) narrows and displaces the cloaca caudally towards the dPCM and the CM. White arrowhead indicates the relative immobility of the dPCM. (P and Q) Developmental defects such as hyperplastic growth of dPCM (large red arrowhead in P, the schematics of G) and agenesis of ICM, GTM and dPCM (small yellow arrowhead in Q, the schematics of K) cause imperforate anus and persistent cloaca, respectively.

proposed occlusion model takes into consideration of all the mesenchymal tissues surrounding the cloaca, including ICM, GTM, dPCM and vPCM, as well as the CM epithelial tissue (Fig. 4M–O). Using somite position as a point of reference, we show for the first time that the dPCM marks the caudal boundary of the cloaca and perhaps more importantly, the dPCM remains stationary while other surrounding tissues grow caudally towards or rotate around the dPCM (Fig. 4M–O). While contributions from all the surrounding tissues are needed, the dPCM plays a central role as the caudal boundary of the cloaca and an anchor of the CM.

We also show that abnormal development of the dPCM correlates to the cloaca malformation in mouse mutants (Fig. 4P and Q). *Dkk1*, a potent inhibitor of the *Wnt/·-catenin* signal pathway, is highly enriched in the dPCM and *Dkk1* mutants exhibit an imperforate anus phenotype (Guo et al., 2014). Results from the 3-D

analyses demonstrate that *Dkk1* signal is critical for the dPCM development but is largely dispensable for formation of other cloaca mesenchyme, including the ICM and the GTM at e11.5. Therefore, *Dkk1* regulates cloacal morphogenesis by regulating formation of the dPCM (Fig. 4P). We have observed that the CM is much shorter in *Dkk1* mutants (Figs. 4E, S6 and S8) (Guo et al., 2014). A similar finding has been reported in other mutants with anorectal malformations (Kluth et al., 1995; Liu et al., 2003; Nakata et al., 2009; Suda et al., 2011; van der Putte, 1986). However, it remains to be determined whether the CM anomaly is a cause or consequence of the dPCM defects in these mutants. *Shh* is specifically expressed in the cloaca epithelium and *Shh* deletion causes a persistent cloaca phenotype (Lin et al., 2009; Miyagawa et al., 2009; Mo et al., 2001; Seifert et al., 2009). In contrast to *Dkk1*, *Shh* is required for growth of all surrounding mesenchyme, including

ICM, dPCM and GTM (Fig. 4). In the absence of *Shh,* these tissues are formed initially at e10.5 but become hypoplastic at e11.5. Therefore, *Shh* signal is an essential growth factor for mesenchymal cells surrounding the cloaca (Fig. 4Q). Consistently, knockout of both *Gli2* and *Gli3,* downstream effectors of the *Shh* signal pathway that are strongly expressed in the cloaca mesenchyme, causes persistent cloaca phenotype similar to *Shh* knockout mutant (Mo et al., 2001). Surprisingly, knockout of *Gli2* alone results in an imperforate anus phenotype; and *Gli3* single mutants have anal stenosis phenotype, suggesting that *Gli2* and *Gli3* have common as well as tissue-specific roles in cloaca mesenchyme (Mo et al., 2001).

Collectively, we propose that coordinated growth and reposition of caudal mesenchymal structures toward the dPCM change the overall spatial relationship surrounding the cloaca. This coordinated process results in occlusion rather than septation of the cloaca (Fig. 4M–O). We suspect that formation of the dPCM might be linked to formation of the CM and cessation of gastrulation (Gruneberg, 1956; Ohta et al., 2010), but future studies are needed to uncover the underlying mechanism.

Acknowledgment

Appendix A. Supplementary material

Supplementary data associated with this article can be found in the online version at http://dx.doi.org/%2010.1016/j.ydbio.2015.10.018.

References

Gruneberg, H., 1956. A ventral ectodermal ridge of the tail in mouse embryos. Nature 177, 787–788.

Guo, C., Sun, Y., Guo, C., MacDonald, B.T., Borer, J.G., Li, X., 2014. Dkk1 in the pericloaca mesenchyme regulates formation of anorectal and genitourinary tracts. Dev. Biol. 385, 41–51.

Hassoun, R., Schwartz, P., Rath, D., Viebahn, C., Manner, J., 2010. Germ layer differentiation during early hindgut and cloaca formation in rabbit and pig embryos. J. Anat. 217, 665–678.

Hynes, P.J., Fraher, J.P., 2004. The development of the male genitourinary system. I. The origin of the urorectal septum and the formation of the perineum. Br. J. Plast. Surg. 57, 27–36.

Kluth, D., Fiegel, H.C., Geyer, C., Metzger, R., 2011. Embryology of the distal urethra and external genitals. Semin. Pediatr. Surg. 20, 176–187.

Kluth, D., Hillen, M., Lambrecht, W., 1995. The principles of normal and abnormal hindgut development. J. Pediatr. Surg. 30, 1143–1147.

Lin, C., Yin, Y., Long, F., Ma, L., 2008. Tissue-specific requirements of {beta}-catenin in external genitalia development. Development 135, 2815–2825.

Lin, C., Yin, Y., Veith, G.M., Fisher, A.V., Long, F., Ma, L., 2009. Temporal and spatial dissection of Shh signaling in genital tubercle development. Development 136, 3959–3967.

Liu, Y., Sugiyama, F., Yagami, K., Ohkawa, H., 2003. Sharing of the same embryogenic pathway in anorectal malformations and anterior sacral myelomeningocele formation. Pediatr. Surg. Int. 19, 152–156.

Miyagawa, S., Moon, A., Haraguchi, R., Inoue, C., Harada, M., Nakahara, C., Suzuki, K., Matsumaru, D., Kaneko, T., Matsuo, I., Yang, L., Taketo, M.M., Iguchi, T., Evans, S. M., Yamada, G., 2009. Dosage-dependent hedgehog signals integrated with Wnt/beta-catenin signaling regulate external genitalia formation as an appendicular program. Development 136, 3969–3978.

Mo, R., Kim, J.H., Zhang, J., Chiang, C., Hui, C.C., Kim, P.C., 2001. Anorectal malformations caused by defects in sonic hedgehog signaling. Am. J. Pathol. 159, 765–774.

Mohun, T.J., Weninger, W.J., 2012a. Episcopic three-dimensional imaging of embryos. Cold Spring Harb. Protoc. 2012, 641–646.

Mohun, T.J., Weninger, W.J., 2012b. Generation of volume data by episcopic three-dimensional imaging of embryos. Cold Spring Harb. Protoc. 2012, 681–682.

Muller, F., O'Rahilly, R., 2004. The primitive streak, the caudal eminence and related structures in staged human embryos. Cells Tissues Organs 177, 2–20.

Nakata, M., Takada, Y., Hishiki, T., Saito, T., Terui, K., Sato, Y., Koseki, H., Yoshida, H., 2009. Induction of Wnt5a-expressing mesenchymal cells adjacent to the cloacal plate is an essential process for its proximodistal elongation and subsequent anorectal development. Pediatr. Res. 66, 149–154.

Nievelstein, R.A., van der Werff, J.F., Verbeek, F.J., Valk, J., Vermeij-Keers, C., 1998. Normal and abnormal embryonic development of the anorectum in human embryos. Teratology 57, 70–78.

Ohta, S., Schoenwolf, G.C., Yamada, G., 2010. The cessation of gastrulation: BMP signaling and EMT during and at the end of gastrulation. Cell Adhes. Migr. 4, 440–446.

Paidas, C.N., Morreale, R.F., Holoski, K.M., Lund, R.E., Hutchins, G.M., 1999. Septation and differentiation of the embryonic human cloaca. J. Pediatr. Surg. 34, 877–884.

Penington, E.C., Hutson, J.M., 2003. The absence of lateral fusion in cloacal partition. J. Pediatr. Surg. 38, 1287–1295.

Rathke, H., 1832. Abhandlungen zur Bildungs- und Entwicklungsgeschichte der Tiere. Leipzig. http://dx.doi.org/http://digital.onb.ac.at/OnbViewer/viewer.faces?doc=ABO_%2BZ167682503.

Seifert, A.W., Bouldin, C.M., Choi, K.S., Harfe, B.D., Cohn, M.J., 2009. Multiphasic and tissue-specific roles of sonic hedgehog in cloacal septation and external genitalia development. Development 136, 3949–3957.

Seifert, A.W., Harfe, B.D., Cohn, M.J., 2008. Cell lineage analysis demonstrates an endodermal origin of the distal urethra and perineum. Dev. Biol. 318, 143–152.

Suda, H., Lee, K.J., Semba, K., Kyushima, F., Ando, T., Araki, M., Araki, K., Inomata, Y., Yamamura, K., 2011. The Skt gene, required for anorectal development, is a candidate for a molecular marker of the cloacal plate. Pediatr. Surg. Int. 27, 269–273.

Tam, P.P., 1981. The control of somitogenesis in mouse embryos. J. Embryol. Exp. Morphol. 65 Suppl, 103–128.

Tourneux, F., 1888. Sur les premiers developpements du cloaque du tubercle genitale et de l'anus chez l'embryon de mouton. J. Anat. 24, 503–517.

van der Putte, S.C., 1986. Normal and abnormal development of the anorectum. J. Pediatr. Surg. 21, 434–440.

Wang, C., Gargollo, P., Guo, C., Tang, T., Mingin, G., Sun, Y., Li, X., 2011. Six1 and Eya1 are critical regulators of peri-cloacal mesenchymal progenitors during genitourinary tract development. Dev. Biol. 360, 186–194.

Wang, C., Wang, J., Borer, J.G., Li, X., 2013. Embryonic origin and remodeling of the urinary and digestive outlets. Plos. One 8, e55587.

Wilson, V., Beddington, R.S., 1996. Cell fate and morphogenetic movement in the late mouse primitive streak. Mech. Dev. 55, 79–89.